Clin Exp Metastasis (2014) 31:87–100
DOI 10.1007/s10585-013-9613-6

RESEARCH PAPER

Role of L1 cell adhesion molecule (L1CAM) in the metastatic cascade: promotion of dissemination, colonization, and metastatic growth

Dirk Weinspach · Bastian Seubert · Susanne Schaten · Katja Honert · Susanne Sebens · Peter Altevogt · Achim Krüger

Received: 27 March 2013 / Accepted: 15 August 2013 / Published online: 4 September 2013

Abstract Expression of the L1 cell adhesion molecule (L1CAM) is frequently increased in cancer patients compared to healthy individuals and also linked with bad prognosis of solid tumours. Previously, we could show that full-length L1CAM promotes metastasis formation via upregulation of gelatinolytic activity in fibrosarcoma. In this study, we aimed to extend this finding to haematogenous malignancies and carcinomas, and to specifically elucidate the impact of L1CAM on major steps of the metastatic cascade. In a well-established T-cell lymphoma spontaneous metastasis model, silencing of L1CAM significantly improved survival of the mice, while intradermal tumour growth remained unaltered. This correlated with significantly decreased spontaneous metastasis formation. L1CAM suppression abrogated the metastatic potential of T-cell lymphoma as well as carcinoma cells as demonstrated by reduced migration and invasion in vitro and reduced formation of experimental metastasis in vivo. At the molecular level, silencing of L1CAM led to reduced expression of gelatinases MMP-2 and -9 in vitro and decreased gelatinolytic activity in primary tumours and metastases in vivo. In accordance, knock down of L1CAM had similar suppressive effects on migration, invasion and in vivo-gelatinolytic activity as treatment with the specific gelatinase inhibitor SB-3CT. This newly discovered impact of L1CAM on distinct steps of the metastatic cascade and MMP activity highlights the potential of possible L1CAM-directed therapies to inhibit metastatic spread.

Keywords L1CAM · Metastatic cascade · Dissemination · Metastatic growth · MMPs · Targeted therapy

Abbreviations

CAM	Cell adhesion molecule
DAPI	4′,6-Diamidino-2-phenylindole
DMSO	Dimethyl sulfoxide
IgSF	Immunoglobulin superfamily
i.d.	Intradermal
i.v.	Intravenous
L1CAM	L1 cell adhesion molecule
MMP-2	Matrix metalloproteinase-2
MMP-9	Matrix metalloproteinase-9
PCNA	Proliferating cell nuclear antigen
PE	Phycoerythrin
shRNA	Short hairpin RNA
X-Gal	5-Bromo-4-chloro-indolyl-β-D-galactopyranoside

Electronic supplementary material The online version of this article (doi:10.1007/s10585-013-9613-6) contains supplementary material, which is available to authorized users.

Dirk Weinspach and Bastian Seubert have contributed equally to this work.

D. Weinspach · B. Seubert · S. Schaten · K. Honert · A. Krüger (✉)
Institute for Experimental Oncology and Therapy Research, Klinikum rechts der Isar, Technische Universität München, 81675 Munich, Germany
e-mail: achim.krueger@lrz.tu-muenchen.de

S. Sebens
Institute for Experimental Medicine, UKSH, Campus Kiel, 24105 Kiel, Germany

P. Altevogt
Translational Immunology Unit (D015), German Cancer Research Center, 69120 Heidelberg, Germany

Introduction

Metastasis is the decisive prognostic parameter in almost all neoplastic malignancies. In fact, nearly 90 % of cancer patients die due to the formation of metastasis [1]. For tumours of epithelial origin, formation of metastases requires tumour cells to complete the multi-step process of the metastasis cascade, including dissemination from the primary tumour, extravasation, formation of micrometastases and re-initiation of tumour cell proliferation [2, 3]. In contrast, dissemination of non-solid tumours, e.g. lymphoma, is thought to follow different rules, and is more likely a consequence of conserved physiological behaviour [4]. Therapeutic strategies applicable for both, solid and non-solid tumours, would therefore be very powerful tools in the war on cancer.

Matrix metalloproteinases (MMPs) are critical mediators of tumour progression and metastasis due to their ability to change the microenvironment in close vicinity to tumour cells [5]. Within the class of MMPs especially the gelatinases MMP-2 and MMP-9 are prominent drivers of tumour progression and metastasis [6, 7] as these pro-metastatic MMPs are pivotal for invasion across basement membranes [8] and also cell migration [9–11]. Previously, we could demonstrate that MMP-2 and MMP-9 are important factors for efficient liver metastasis formation of a murine T-lymphoma cell line [12]. Consequently, pharmacological interference with MMP-2 and MMP-9, employing the highly specific gelatinase inhibitor SB-3CT [13], was shown to be effective in inhibiting liver metastasis formation [14], demonstrating the significance of gelatinases for metastases formation of a non-solid tumour. Based on the importance of proteases during metastasis formation, it is fundamental to understand their regulation during tumour progression.

The activity of matrix metalloproteinases is regulated by different classes of molecules including growth factors, cytokines [15], integrins [16] and cell adhesion molecules [17]. The involvement of cell adhesion molecules of the immunoglobulin superfamily (IgSF CAMs) in all steps of the metastatic cascade is well established [18–20]. One of the best studied members of the IgSF CAMs is the L1 cell adhesion molecule (L1CAM) [21, 22]. Elevated expression of L1CAM in different tumour entities including uterine and ovarian carcinoma correlates with short survival [23], and is linked to liver metastasis formation in patients as well as in mouse tumour models [24–28]. These findings have motivated interfering strategies employing antibodies [29–31] and shRNAs (short hairpin RNAs) [32, 33] directed against L1CAM, resulting in reduced tumour growth and metastasis formation. However, the precise function of L1CAM during distinct steps of the metastatic cascade is still unclear.

In order to investigate the consequence of functional interference with L1CAM on tumour cell motility, dissemination, and metastatic colony formation of a non-solid tumour, we used the well-established L-CI.5s T-lymphoma metastasis model. Employing this model, we here demonstrate that L1CAM is important for tumour cell dissemination from the primary tumour and tumour cell outgrowth at the site of metastasis by altering MMP expression and gelatinolytic activity. We could broaden these findings to a typical L1CAM-dependent solid tumour entity employing an ovarian carcinoma metastasis model. Together, these findings indicate L1CAM as a decisive factor for metastasis formation of solid and non-solid tumours and emphasise L1CAM as a valuable therapeutic target in the restriction of metastatic spread.

Materials and methods

Cells and viruses

The murine T-lymphoma cell line L-CI.5s is a *lacZ*-tagged variant of ESb lymphoma cells, which were originally obtained upon re-isolation of intradermally inoculated ESb lymphoma cells from liver metastases [34]. The human ovarian carcinoma cell line SKOV3ip-*lacZ* is a lacZ-tagged variant of SKOV3ip ovarian carcinoma cells. 293T, L-CI.5s [34], and SKOV3ip-*lacZ* cells [29] were cultured as described previously. For generation of a stable L1CAM knockdown in L-CI.5s and SKOV3ip-*lacZ* cell lines shRNAi technology was used. Potential shRNA target sequences of a length of 19–22 bp within the L1CAM sequence were identified using the program shRNA *target finder* (Ambion/Life Technologies, Darmstadt, Germany) and checked for potential off-target effects using the BLAST algorithm (http://blast.ncbi.nlm.nih.gov/Blast.cgi). shRNA oligonucleotides targeting murine L1CAM (shL1–2: 5′-AACAAATATGGTCCTGGAGAA-3′, shL1-3: 5′-AAGCCACATAGTGGTACCTGC-3′) and shRNA oligonucleotides targeting human L1CAM (shL1-2: 5′-AAGTACCGGATTCAGCGTGGC-3′, shL1-3: 5′-AACTTCGGACACACAACCTGA-3′) were designed containing a 5′-*Bam*HI overhang and a 3′-*Eco*RI overhang and aligned into the retroviral shRNA vector pSIREN-RetroQ (Clontech/Takara Bio Europe, Saint-Germain-en-Laye, Frankreich). Recombinant retroviruses were generated by transient transfection of 293T cells with 10 mg pHIT60 [35], 10 mg pHCMV-G [36] and 10 mg of pSIREN-RetroQ-shscr or pSIREN-RetroQ-shL1, respectively. Retroviral transduction was performed as described previously [37]. Transduction of adherent cells was performed using viral supernatant and transduction of the suspension cell

line L-CI.5s was performed by co-culture with virus-producing 293T cells for 48 h.

Animal experiments

Spontaneous metastasis assay

1×10^6 L-CI.5s cells (resuspended in PBS) were intradermally inoculated into pathogen-free, syngeneic, female DBA/2 mice (Charles River, Sulzfeld, Germany). Tumour take was 100 % and comparable in size in all mice. Primary tumour growth was constantly monitored by visual inspection and measured using a calliper gauge. In one experiment mice were sacrificed when showing first signs of morbidity due to severe metastatic disease (day 11 after tumour cell inoculation (a.t.c.i.)) according to the animal welfare guidelines of the Tierschutzgesetz des Freistaates Bayern and approved by the *Regierung von Oberbayern*. In a second experiment mice were sacrificed, when the first tumours had reached a size of 1.0 mm in diameter (day 8 a.t.c.i.). At sacrifice, portions of tumours were snap-frozen and stored in liquid nitrogen, embedded with TissueTek® or were fixed in 4 % buffered formalin for routine histopathologic processing. For quantification of macrometastatic foci, livers and lungs were stained with X-Gal (5-bromo-4-chloro-3-indolyl-*b*-D-galactopyranoside) (Fermentas, St. Leon-Rot, Germany) as described previously [34, 38]. All foci on the surface of the left lung lobe and foci >0.2 mm on the surface of the median liver lobes were counted.

Experimental metastasis assays

5×10^3 L-CI.5s were inoculated into the tail vein of pathogen-free, syngeneic, female DBA/2 mice (Charles River, Sulzfeld, Germany). 1×10^6 SKOV3ip-*lacZ* cells were analogously inoculated into pathogen-free, athymic, female $CD1^{nu/nu}$ mice (Charles River, Sulzfeld, Germany). Mice were sacrificed 7 days (L-CI.5s) or 26 days (SKOV3ip-lacZ) after tumour cell inoculation. For quantification of macrometastatic foci, livers or lungs were stained with X-Gal as described above. All foci on the surface of the left lung lobe and foci >0.2 mm on the surface of the median liver lobes were counted.

Ethics statement

All animal experiments were performed in compliance with the guidelines of the Tierschutzgesetz des Freistaates Bayern and approved by the *Regierung von Oberbayern* (permission number: 55.2-1-54-2531-69-05; 55.2-1-54-2531-13-09) and all efforts were made to minimize suffering.

In vitro assays

Alternatively, analysis of cell viability/proliferation was performed by seeding of 2×10^3 cells/well in 96 well plates, and quantification of the number of living cells at the indicated time points after seeding using the AlamarBlue® proliferation assay (Invitrogen, Darmstadt, Germany) according to the manufacturer's protocol. Transwell migration assays were performed using Costar Transwell Permeable Supports with 3 μm (L-CI.5s) and 8 μm (SKOV3ip-*lacZ*) pore size (Corning Inc., Corning, NY, USA). 2×10^4 SKOV3ip-*lacZ* cells and 1×10^5 L-CI.5s cells, respectively, were seeded in serum-free media. Media containing 10 % FCS (Biochrom, Berlin, Germany) were used as chemoattractant added to the bottom chamber of 24 well plates. After an incubation time of 12 h (SKOV3ip-*lacZ*) and 48 h (L-CI.5s) at 37 °C, non-invasive cells were removed using a cotton stick and invaded cells were fixed using Diff-Quik solution (Dade Behring, Marburg, Germany) and stained using DAPI (AppliChem, Darmstadt, Germany).

Matrigel invasion assays were performed using Costar Transwell Permeable Supports with 3 μm (L-CI.5s) and 8 μm (SKOV3ip-*lacZ*) pore size coated with 1 mg/mL BD Matrigel™ Basement Membrane Matrix (BD Biosciences, Heidelberg, Germany). 1×10^5 SKOV3ip-*lacZ* cells and 5×10^5 L-CI.5s cells, respectively, were seeded in serum-free media. Media containing 10 % FCS were used as chemoattractant added to the bottom chamber of 24 well plates. After an incubation time of 48 h at 37 °C, non-invasive cells were removed using a cotton stick and invaded cells were fixed using Diff-Quik solution and stained using DAPI.

RNA isolation, reverse transcription, and qRT-PCR

According to the manufactures' protocols, RNA isolation from cell lines was performed using TRIzol-Reagent (Life Technologies, Darmstadt, Germany) and RNA isolation from murine lung and liver tissues as well as from human primary tumours and metastases was done with RNeasy Midi Kit (Qiagen, Hilden, Germany) after harvesting the snap-frozen tissues. Reverse transcription and qRT-PCR were performed as described previously [39]. Gene expression analysis was performed using two different approaches. (1) TaqMan® Gene Expression Assays (Applied Biosystems, Darmstadt, Germany) were used for quantification of the following genes: human L1CAM (Hs00240928_m1), human MMP-2 (Hs00234422_m1), human MMP-9 (Hs00234579_m1), murine L1CAM (Mm00493049_m1), murine MMP-2 (Mm00439508_m1), murine MMP-9 (Mm00600163_m1), murine PCNA (Mm00448100_g1), and lacZ (LACZ1-LAC3). Data was normalised to human 18S rRNA (4319413E, RefSeq: X03205.1). (2) Designed qRT-PCR

assays using Universal ProbeLibrary Set, Human (04683633001) and Universal ProbeLibrary Set, Mouse (04683641001) (Roche, Penzberg, Germany) in combination with gene-specific primers. Primer sequences were obtained using the Universal ProbeLibrary Assay Design Center (https://www.roche-applied-science.com/sis/rtpcr/upl/index.jsp?id=UP030000). The following genes were quantified using this approach using the following assays: human MMP-2 (Probe #34), human MMP-9 (Probe #24), human MT1-MMP (Probe #83), murine MMP-2 (Probe #85), murine MMP-9 (Probe #19), and murine MT1-MMP (Probe #42).

Immunoprecipitation and western blot analysis

For detection of murine L1CAM on protein level, L1CAM was immunoprecipitated from cell lysates of L-CI.5s cells. Briefly, 1 µg mouse monoclonal anti-human L1CAM antibody L1-14.10 was bound to Protein G Sepharose. After binding of the antibody to Protein G Sepharose, cell lysates containing 1 mg total protein were added and incubated on a tube rotator for overnight at 4 °C. Immunoprecipitation samples were applied to western blot analysis.

For western blot analysis, 40 µg of protein were electrophoresed through 10 % SDS-PAGE and electroblotted at 12 V for 75 min. Blots were blocked with 5 % BSA in TBST for at least 1 h at RT. Antibodies used were mouse monoclonal anti-human L1CAM antibody L1-9.3 (diluted at 1 µg/mL in 5 % BSA/TBST), mouse monoclonal anti-human L1CAM antibody L1-14.10 (substantial cross-reactivity against murine L1CAM; diluted at 1 µg/mL in 5 % BSA/TBST), and anti-α-tubulin mouse mAb DM1A (Calbiochem, Merck, Darmstadt, Germany; diluted 1:2000 in 5 % BSA/TBST). Anti-L1CAM antibodies were kindly provided by Dr. Peter Altevogt (DKFZ Heidelberg, Germany). Incubation with all primary antibodies was performed overnight at 4 °C, followed by detected with ECL mouse IgG, HRP-linked whole Ab (GE Healthcare Europe GmbH, Freiburg, Germany; diluted 1:2000 in 5 % BSA/TBST), and visualisation by Clarity ECL Western Substrate (Bio-Rad Laboratories GmbH, München, Germany). Image acquisition was performed using Molecular Imager ChemiDoc XRS System and Image Lab version 4.0 software (Bio-Rad Laboratories GmbH, München, Germany).

Flow cytometric analysis

L1CAM expression on L-CI.5s and SKOV3ip-*lacZ* cells was performed using flow cytometry. Briefly, 1×10^5 cells were stained using either monoclonal rat anti-mouse L1CAM antibody, clone 555 (L-CI.5s) and monoclonal mouse anti-human L1CAM antibody L1-9.3/2a (SKOV3ip-*lacZ*) (kindly provided by Dr. Peter Altevogt, DKFZ Heidelberg, Germany), followed by Goat polyclonal Secondary Antibody to Rat IgG–H&L (PE) (ab97058, Abcam, Cambridge, UK) and PE Goat anti-mouse IgG (minimal x-reactivity) (#405307, BioLegend, London, UK) secondary antibodies, respectively. Flow cytometric analysis was performed using BD FACSCanto II flow cytometer (BD Biosciences, Heidelberg, Germany), and data was analysed using FlowJo v8 software (Tree Star, Inc., Ashland, OR, USA).

In situ zymography

For in situ zymography, tumour tissue samples, metastases-bearing liver or lung samples, respectively, were embedded in Tissue-TekH O.C.T^{TM} Compound (Sakura Finetek, Staufen, Germany) and shock-frozen on dry-ice. In situ zymography was performed as reported previously [14]. Images were taken using Nikon ECLIPSE TE2000-S microscope and NIS Elements BR 3.10 software (Nikon Instruments Europe, Badhoevedorp, The Netherlands).

X-Gal staining of cryo sections

For the visualisation of *lacZ*-tagged tumour cells in primary tumour tissue and liver metastases, X-Gal staining was performed on cryo sections. Briefly, cryo sections were fixed for 10 min in Fixation solution (2 % formaldehyde, 0.2 % glutaraldehyde in PBS), washed 10 min in wash solution (2 mM $MgCl_2$ in PBS) and 10 min in detergent solution (2 mM $MgCl_2$, 0.01 % sodium deoxycholate, 0.02 % Nonidet-P40). Afterwards, cryo sections were incubated with X-Gal staining solution for 6 h at 37 °C, washed with PBS and counter-stained by performing HE staining. Images were taken using Leica DMR microscope (Leica Microsystems, Wetzlar, Germany) and SPOT Advanced Software (SPOT Imaging Solutions, Sterling Heights, MI, USA).

Immunohistochemical PCNA staining

Fixed sections of livers of the different groups were paraffin embedded for immunostaining. Dewaxing, rehydration, blocking, and antigen retrieval of liver sections (4 µm) were done as described [39]. Sections were incubated with Rabbit polyclonal antibody to PCNA (1:2,000) (Abcam, Cambridge, UK) for 20 h at 4 °C and washed in TBS, 0.1 % (v/v) Tween 20. Detection of the bound primary antibody was performed using the Cell and Tissue Staining Kit (R&D Systems, Wiesbaden-Nordenstadt, Germany) and 3,3′-diaminobenzidine (DAB) substrate (DAKO Liquid DAB+ Substrate-Chromogen Solution, DAKO Deutschland, Hamburg, Germany) were used for detection. Sections were counterstained with Mayer's hemalum (Merck, Darmstadt, Germany). Images were taken using Leica DMR microscope (Leica Microsystems, Wetzlar, Germany) and SPOT Advanced Software (SPOT Imaging Solutions, Sterling Heights, MI, USA).

Statistical analysis

Normal distribution of data was tested using the Kolmogorov–Smirnov test and equal variance was tested using Levene-Median test. Two group experiments with normally distributed data were analysed by unpaired *t*-test (Figs. 1a, e, f, 2f, 3b, c, 4a, b, 6a, g, h; Suppl. Figs. 1a, e–h, 3a) with non-normally distributed data were analysed by Mann–Whitney Rank Sum test (Fig. 2e). Three or more group experiments with normally distributed data were statistically analysed by one way analysis of variance (ANOVA) (Figs. 5b, 6d, e; Suppl. Figs. 1j, 3d) and subsequent post hoc comparison applying the Holm–Sidak method (Figs. 5b, 6d; Suppl. Figs. 1j, 3d). Three group experiments with non-normally distributed data were statistically analysed by Kruskal–Wallis analysis of variance (ANOVA) on Ranks (Fig. 5a; Suppl. Figs. 1i, 3e) and subsequent post hoc comparison by applying the Dunn's method (Fig. 5a; Suppl. Figs. 1i, 3e). Statistic significance was indicated according to the Michelin Guide scale: $p < 0.05$ (*, significant), $p < 0.01$ (**, highly significant), and $p < 0.001$ (***, extremely significant).

All statistical analyses were performed using SigmaStat for Windows Software version 3.00 (SPSS Inc./IBM, Armonk, NY, USA). Kaplan–Meier survival analysis and log-rank test for statistical significance of the survival data were performed using GraphPad Prism Software version 6.0.1 (GraphPad Software Inc., San Diego, CA, USA).

Results

Tumour cell-derived L1CAM is an important regulator of the metastatic potential and inversely correlates with survival

In order to investigate the contribution of L1CAM to the metastatic potential of non-solid tumours, we transduced the murine T-lymphoma cell line L-CI.5s with retroviral vectors expressing shRNAs against L1CAM. Knock down of

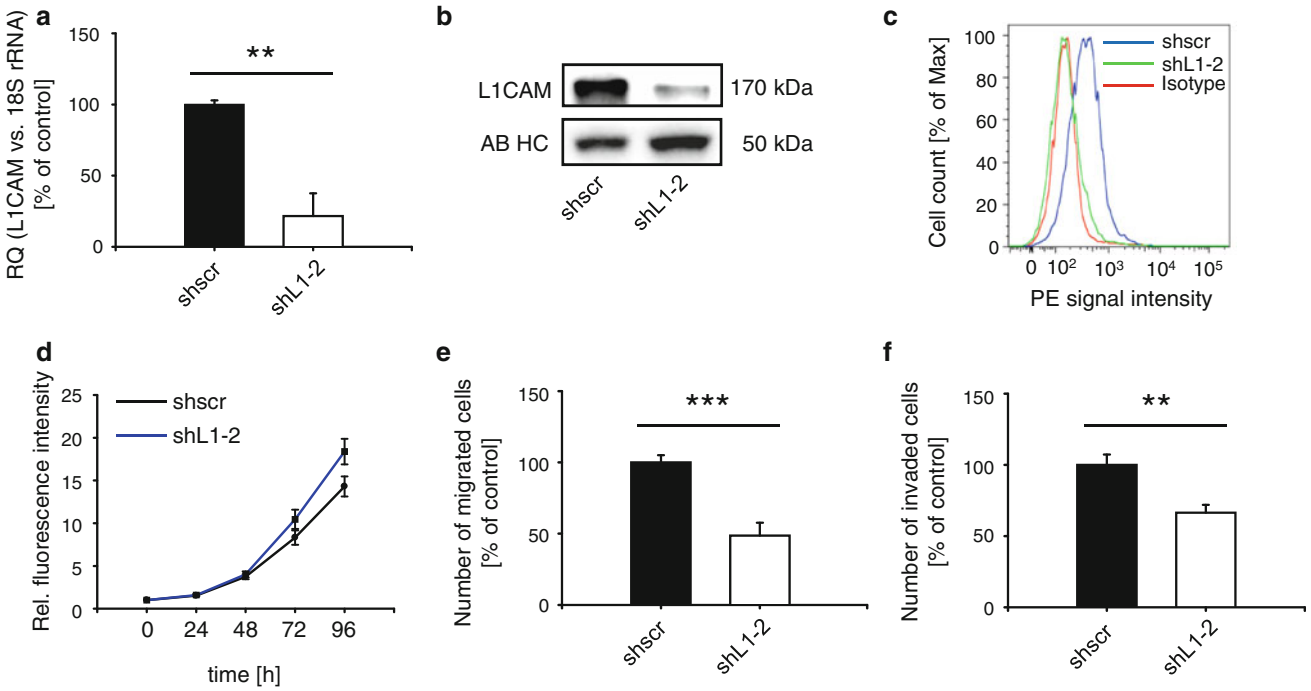

Fig. 1 Tumour cell-derived L1CAM expression is an important regulator of the metastatic potential in vitro. L-CI.5s cells were transduced with retroviruses containing a shRNA sequence directed against murine L1CAM (shL1-2) or with a non-targeting shRNA sequence (shscr, scrambled shRNA). **a** TaqMan® analysis revealed significantly reduced L1CAM expression in L-CI.5s cells. Mean expression of L1CAM mRNA ± SEM (*columns* ± *bars*) in L-CI.5s cells. L1CAM mRNA expression levels were normalised to 18S rRNA levels and the mean of the reference group (*shscr*) was set as 100 % ($n = 3$; shL1-2 vs. shscr: $^{**}p = 0.001$, as determined by unpaired *t* test). **b** Western blot analysis of immunoprecipitated L1CAM revealed that L1CAM protein levels were significantly reduced in L-CI.5s cells. **c** Flow cytometric analysis revealed that L1CAM expression was significantly reduced in L-CI.5s cells. **d** For analysis of cell viability/proliferation, 2×10^3 cells/well were seeded in 96 well plates, and the number of living cells was quantified 0, 24, 48, 72 and 96 h after seeding using the AlamarBlue® proliferation assay ($n = 6$). **e** Mean number of migrated cells per image section ± SEM (*columns* ± *bars*) for the different L-CI.5s cells as analysed by trans-well migration assay. The mean of the reference group (*shscr*) was set as 100 % ($n = 6$; shL1-2 vs. shscr: $^{***}p \leq 0.001$, as determined by unpaired *t*-test). **f** Mean number of invaded cells per image section ± SEM (*columns* ± *bars*) for the different L-CI.5s cells as analysed by Matrigel invasion assay. The mean of the reference group (*shscr*) was set as 100 % ($n = 6$; shL1-2 vs. shscr: $^{**}p = 0.003$, as determined by unpaired *t*-test)

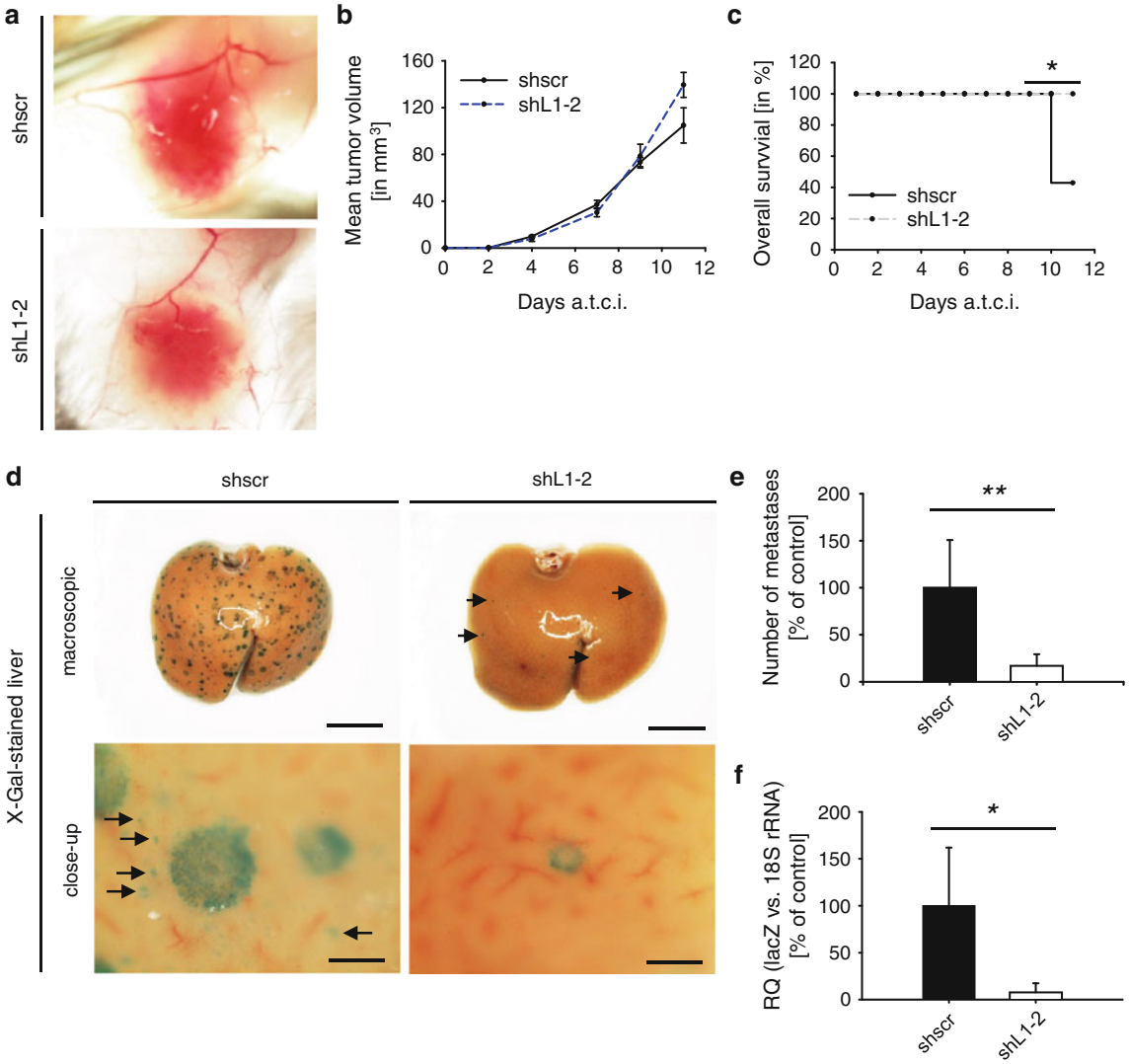

Fig. 2 Tumour cell-derived L1CAM expression is an important regulator of the metastatic potential in vivo and inversely correlated with survival. **a–c** 1×10^6 of the different L-CI.5s cells were inoculated on day zero and tumour diameter was monitored by tumour diameter measurements from days 2 to 11 using a calliper. Mice were sacrificed when showing first signs of morbidity. **a** Representative tumours of each group are shown at day 8. **b** Tumour volumes were calculated based on tumour diameter measurements. Mean tumour volume ± SEM (*dots* ± *bars*); shscr: $n = 7$ mice, shL1-2: $n = 6$ mice. **c** A theoretical overall survival was calculated based on the monitored health status of the mice at day 11. Moribund mice were evaluated as dead mice for calculation, and to minimize suffering of the animals (shscr: $n = 7$ mice, shL1-2: $n = 6$ mice; $^*p = 0.033$, as determined by log-rank test). **d** X-Gal staining (*indigoblue foci*) of removed livers. 1×10^6 of the different L-CI.5s cells were inoculated on day zero and tumour diameter was monitored by tumour diameter measurements from days 2 to 8 using a calliper. Eight days after inoculation of the tumour cells DBA/2 mice were sacrificed, and their primary tumours and livers were removed. Representative surface images are presented (*bars:* 5 mm (macroscopic), 0.3 mm (close-up)). **e** Mean number of spontaneous liver metastases ± SEM (*columns* ± *bars*) from the spontaneous metastasis assay. The mean of the reference group (*shscr*) was set as 100 % (shscr: $n = 7$ mice each; shL1-2: $n = 6$ mice; shL1-2 vs. shscr: $^{**}p = 0.003$, as determined by unpaired *t*-test). **f** Mean expression of the bacterial *lacZ* gene ± SEM was normalised to 18S rRNA levels (*columns* ± *bars*) in livers. The mean of the reference group (*shscr*) was set as 100 % (shscr: $n = 7$, shL1-2: $n = 6$; shL1 vs. shscr: $^*p = 0.015$, as determined by Mann–Whitney Rank Sum test)

L1CAM was confirmed on mRNA (Fig. 1a; Suppl. Fig. 1a) and protein level (Fig. 1b, c; Suppl. Fig. 1b, c) employing TaqMan, western blot and flow cytometric analysis. Attenuation of L1CAM had no effect on tumour cell proliferation (Fig. 1d; Suppl. Fig. 1d). Instead, trans-well migration and Matrigel invasion assays significantly demonstrated reduced migratory and invasive capacity of L-CI.5s cells upon L1CAM knock down (Fig. 1e, f; Suppl. Fig. 1e, f).

Next we addressed the question whether the decreased tumour cell motility impacts on the metastatic behaviour in vivo. Therefore, we inoculated L-CI.5s cells intradermally into the flank of syngeneic DBA/2 mice and

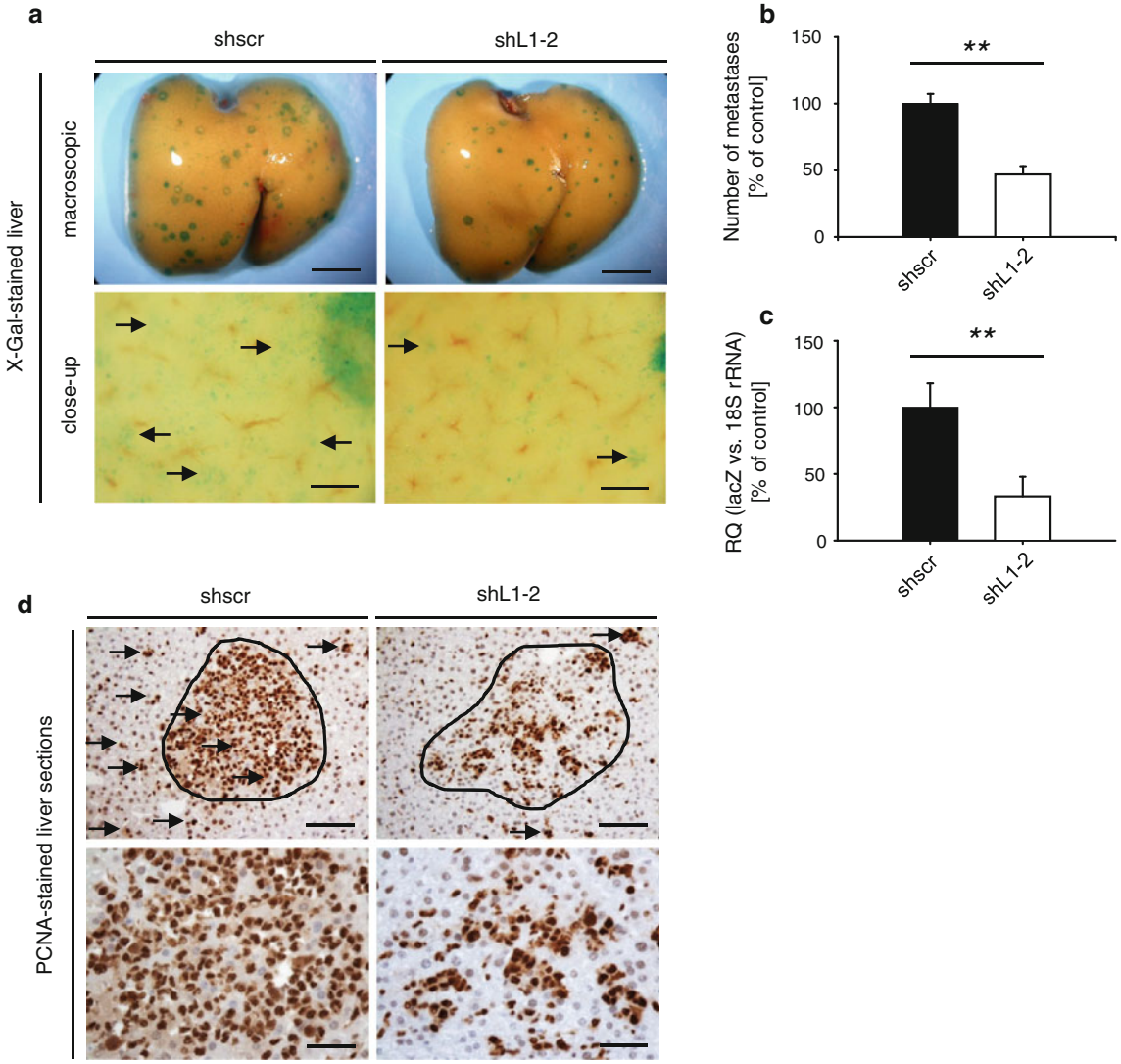

Fig. 3 L1CAM is necessary for metastatic outgrowth and tumour cell proliferation in the liver. **a**–**e** Seven days after inoculation of 5×10^3 of the different L-CI.5s cells, DBA/2 mice were sacrificed, and their livers were removed. **a** X-Gal staining (*indigoblue foci*) of removed livers. Representative surface images are presented *bars* 6 mm (macroscopic), 0.3 mm (close-up). **b** Mean number of liver metastases ± SEM (*columns* ± *bars*). The mean of the reference group (*shscr*) was set as 100 % (shscr: $n = 4$ mice each; shL1-2: $n = 4$ mice; shL1-2 vs. shscr: $^{**}p = 0.001$, as determined by unpaired *t*-test). **c** Mean expression of the bacterial *lacZ* gene in livers ± SEM (*columns* ± *bars*). *lacZ* levels were normalised to 18S rRNA, and the mean of the reference group (*shscr*) was set as 100 % ($n = 4$ mice each; shL1-2 vs. shscr: $^{**}p = 0.001$, as determined by unpaired *t*-test). **d** Immunohistochemical staining of PCNA on paraffin-embedded formalin-fixed liver sections. PCNA expressing cells were stained brown (*bars*: 100 µm (*upper row*), 50 µm (*bottom row*))

monitored primary tumour growth. We found that silencing of L1CAM did not alter intradermal tumour growth (Fig. 2a, b) but significantly increased survival of mice as compared to the shscr control group (Fig. 2c). In accordance, we found that silencing of L1CAM resulted in dramatically reduced spontaneous metastasis to the liver (Fig. 2d). Consistently, the number of metastatic colonies, as revealed by X-Gal staining (Fig. 2e), as well as the overall tumour burden of the liver, as measured by *lacZ* TaqMan (Fig. 2f), were significantly reduced as compared to the shscr control. These findings suggest that tumour cell-derived L1CAM is important for dissemination of tumour cells from the primary tumour and homing to the target organ of metastasis.

L1CAM is necessary for metastatic outgrowth and tumour cell proliferation in the liver

Next, we aimed to determine whether knock down of L1CAM in tumour cells affects colony formation in the target organ of metastasis. In order to specifically monitor colonization of the target organ by tumour cells, we employed an experimental metastasis assay. Remarkably, L1CAM suppression led to significantly reduced numbers

of metastatic colonies (Fig. 3a, b) as revealed by X-Gal staining, while non-injected control livers displayed no X-Gal staining (Suppl. Fig. 2a). Suppression of L1CAM also reduced scattering of tumour cells throughout the liver parenchyma (Fig. 3a, arrows), and total tumour burden of the liver was dramatically reduced upon L1CAM knock down (Fig. 3c).

Next, we addressed the question whether tumour cell proliferation in the target organ of metastasis is affected by L1CAM knock down. In order to distinguish the highly proliferative tumour cells from the surrounding liver parenchyma we employed immunohistochemical PCNA staining of liver sections. Indeed, knock down of L1CAM led to a decreased number of PCNA-positive cells within metastatic foci as compared to the shscr control. Moreover, decreased proliferation of tumour cells within metastatic foci was accompanied by reduced scattering of tumour cells throughout the liver parenchyma (Fig. 3d, arrows). These findings suggest that L1CAM is necessary for the outgrowth of tumour cells in the target organ of metastasis.

L1CAM correlates with increased expression of matrix metalloproteinases in vitro and gelatinolytic activity in vivo

Previously, we reported that tumour cell-derived MMP-2 and MMP-9 are important factors for the metastatic colonisation of the liver [12]. Therefore, we analysed whether L1CAM knock down decreased gelatinase expression. TaqMan analysis revealed significantly decreased MMP-2 (Fig. 4a; Suppl. Fig. 1g) and MMP-9 (Fig. 4b; Suppl. Fig. 1h) expression upon L1CAM knock down. In order to analyse gelatinolytic activity in vivo, we performed gelatine in situ-zymography on primary tumour cryo sections. Areas of tumour tissue and liver metastases were identified by X-Gal staining on representative cryo sections (Suppl. Fig. 2b). We found markedly reduced gelatinase activity in primary tumours of the L1CAM knock down group as compared to the respective control (Fig. 4c). Moreover, L1CAM knock down in the tumour cells led to decreased gelatinolytic activity in liver metastases of mice challenged with tumour cells in spontaneous as well as experimental metastasis assays (Fig. 4d). Collectively, these findings indicate that L1CAM promotes liver metastasis of tumour cells by regulating the expression and activity of pro-metastatic gelatinases.

Specific inhibition of MMP-2 and MMP-9 with the synthetic gelatinase inhibitor SB-3CT mimicks L1CAM knock down phenotype

In order to investigate whether reduced MMP-2 and MMP-9 activity are responsible for the decreased metastatic potential of tumour cells upon L1CAM knock down, we employed the specific gelatinase inhibitor SB-3CT. Incubation experiments revealed that SB-3CT treatment led to decreased trans-well migration and Matrigel invasion, which was comparable to the effects observed upon knock down of L1CAM (Fig. 5a, b; Suppl. Fig. 1i, j). Inhibition of MMP-2 and MMP-9 by SB-3CT did not significantly further reduce cell migration but significantly reduced Matrigel invasion of the shL1 cells.

Next, we investigated whether SB-3CT treatment blocks gelatinolytic activity in vivo. Indeed, we observed that the gelatinolytic activity in primary tumours as well as within liver metastases was decreased upon SB-3CT administration to an extent, which was comparable to the effect of the L1CAM knock down (Fig. 5c). Together, these findings indicate that presence of L1CAM is necessary for gelatinolytic activity of tumour cells in vitro and in vivo.

L1CAM positively regulates the metastatic potential of ovarian carcinoma cells

As a proof of principle that L1CAM mediates metastasis formation via regulation of gelatinase expression, we knocked down L1CAM in a human ovarian carcinoma cell line SKOV3ip, which represents a typical, solid L1CAM-dependent tumour model [23]. Stable suppression of L1CAM in lacZ-tagged SKOV3ip-*lacZ* cells was confirmed by TaqMan (Fig. 6a; Suppl. Fig. 3a), western blot (Fig. 6b; Suppl. Fig. 3b) and flow cytometric analysis (Fig. 6c; Suppl. Fig. 3c). We found significantly reduced tumour cell migration as well as Matrigel invasion upon L1CAM knock down (Fig. 6d, e; Suppl. Fig. 3d, e), while tumour cell proliferation remained unaltered (Fig. 6f; Suppl. Fig. 3f). In accordance with our findings for the

Fig. 4 L1CAM correlates with increased expression of matrix metalloproteinases in vitro and gelatinolytic activity in vivo. **a** Mean MMP-2 mRNA expression ± SEM (*columns* ± *bars*) in the different L-CI.5s cells. MMP-2 levels were normalised to 18S rRNA levels and the mean of the reference group (*shscr*) was set as 100 % ($n = 3$; shL1-2 vs. shscr: $^{**}p = 0.003$, as determined by unpaired *t* test). **b** Mean MMP-9 mRNA expression ± SEM (*columns* ± *bars*) in the different L-CI.5s cells. MMP-9 levels were normalised to 18S rRNA levels and the mean of the reference group (*shscr*) was set as 100 %. ($n = 3$; shL1-2 vs. shscr: $^{*}p = 0.035$, as determined by unpaired *t*-test). **c** In situ zymography was performed on cryo-sections of primary tumours (*left column within each group*) and livers bearing metastases (*right column within each group*) originating from the L-CI.5s spontaneous metastasis assay. Representative images are presented (*bars:* 100 µm; upper row (*green signal*): degraded DQ-gelatine; lower row (*blue signal*): DAPI counter-staining). **d** In situ zymography was performed on cryo-sections of livers bearing metastases originating from the L-CI.5s experimental metastasis assay. Representative images are presented (*bars:* 100 µm; *upper row* (*green signal*): degraded DQ-gelatine; *lower row* (*blue signal*): DAPI counter-staining)

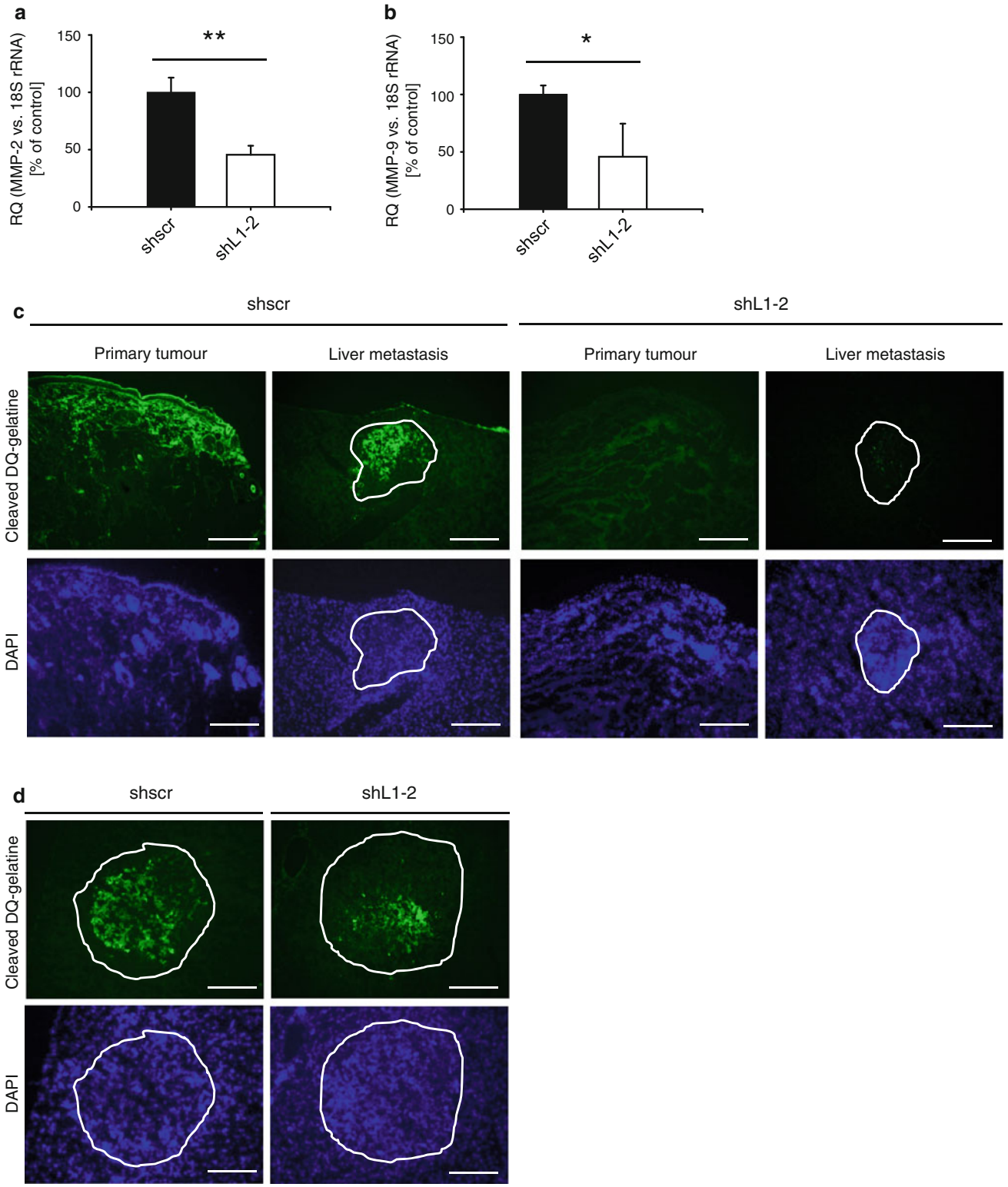

T-cell lymphoma model of non-solid tumours, silencing of L1CAM in SKOV3ip-*lacZ* cells significantly reduced mRNA expression of MMP-2 and MMP-9 (Fig. 6g, h). Strikingly, the gelatinase-specific inhibitor SB-3CT reduced the in vitro migratory and invasive potential of the tumour cells to an extent comparable to the L1CAM knock down (Fig. 6e, f; Suppl. Fig. 3d, e). Finally, experimental lung metastasis was significantly reduced upon knock

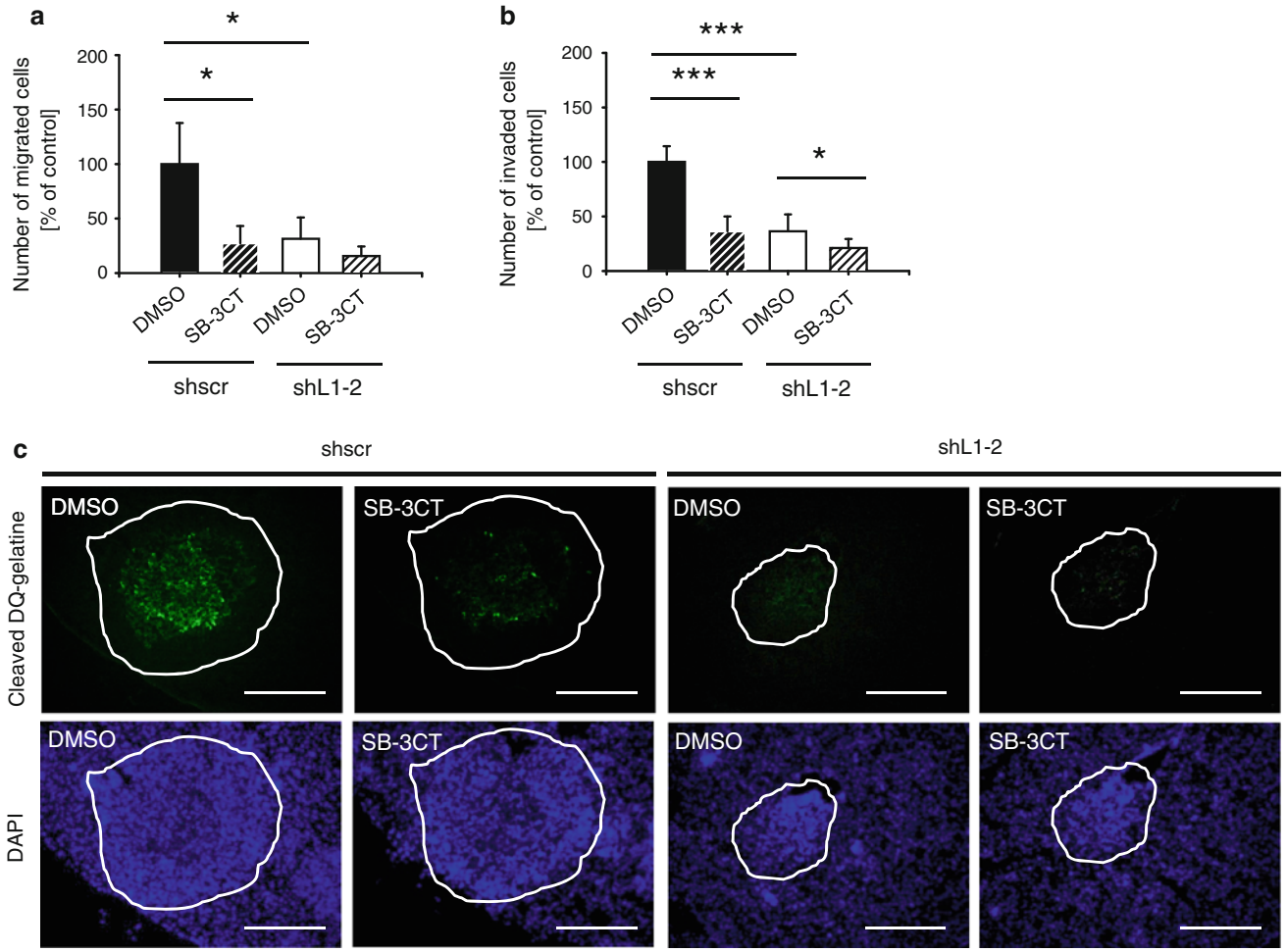

Fig. 5 Specific inhibition of MMP-2 and MMP-9 with the synthetic gelatinase inhibitor SB-3CT mimicks L1CAM knock down phenotype. **a** Mean number of migrated cells per image section ± SEM (*columns* ± *bars*) for the different L-CI.5s cells as determined by trans-well migration assay. Cells were either incubated with 20 μM gelatinase inhibitor SB-3CT or DMSO as a control. The mean of the reference group (*shscr*, *DMSO*) was set as 100 % ($n = 6$ each; all group comparison: $^{**}p \leq 0.001$; shscr, SB-3CT vs. shscr, DMSO: $^{*}p < 0.05$; shL1-2, DMSO vs. shscr, DMSO: $^{*}p < 0.05$; shL1-2, SB-3CT vs. shscr, DMSO: $^{*}p < 0.05$, as determined by Kruskal–Wallis One Way ANOVA on Ranks). **b** Mean number of invaded cells per image section ± SEM (*columns* ± *bars*) for the different L-CI.5s cells as determined by Matrigel invasion assay. Cells were either incubated with 20 μM gelatinase inhibitor SB-3CT or DMSO as a control. The mean of the reference group (*shscr, DMSO*) was set as 100 % ($n = 6$ each; all group comparison: $^{*}p \leq 0.001$, as determined by One Way ANOVA; single group comparison: shscr, SB-3CT vs. shscr, DMSO: $^{***}p < 0.001$; shL1-2, DMSO vs. shscr, DMSO: $^{***}p < 0.001$; shL1-2, SB-3CT vs. shscr, DMSO: $^{***}p < 0.001$; shL1-2, SB-3CT vs. shL1-2, DMSO: $^{*}p = 0.032$; as determined by One Way ANOVA and subsequent post hoc comparison by Holm–Sidak method). **c** In situ zymography was performed on cryo-sections of livers bearing metastases either originating from the L-CI.5s spontaneous metastasis assay. Sections were incubated either with 200 μm SB-3CT (*right column within each group*) or with DMSO as a control (*left column within each group*). Representative images are presented (*bars:* 100 μm; upper row (*green signal*): degraded DQ-gelatine; lower row (*blue signal*): DAPI counter-staining)

down of L1CAM (Fig. 6i, j). Collectively, these findings suggest that L1CAM positively contributes to efficient metastasis formation of solid tumours via up-regulation of pro-metastatic MMP-2 and MMP-9.

Discussion

In this study, we investigated the role of L1CAM during metastasis formation, especially tumour cell dissemination from the primary tumour, colonization, and tumour cell outgrowth at the site of metastasis. We here show for the first time that L1CAM specifically impacts on tumour cell dissemination from the primary tumour as well as metastatic outgrowth in the target organ of metastasis via the regulation of pro-metastatic MMP-2 and MMP-9 in solid and non-solid tumour entities. These findings clearly demonstrate that functional interference with L1CAM is a promising therapeutic approach to specifically inhibit metastatic spread of aggressive solid and non-solid tumours.

We and others could previously show, that antibody-based interference with L1CAM leads to decreased tumour

cell proliferation in vitro [29, 40]. However, the impact of L1CAM knock down on tumour cell proliferation is unclear. While Hung et al. [33] showed decreased tumour cell proliferation upon L1CAM knock down, Hai et al. [32] found that L1CAM knock down does not alter tumour cell proliferation. In accordance to Hai et al., we here demonstrate that L1CAM knock down did not impact on tumour cell proliferation, indicating that it is important to analyse the effects of L1CAM on tumour cell proliferation in a context-dependent manner. Subsequent in vivo-studies have demonstrated that over-expression of L1CAM promotes ectopic tumour growth of ovarian carcinoma [41, 42], while suppression of L1CAM reduces tumour growth in orthotopic tumour models [32, 33, 43]. In contrast to these studies, we demonstrate that silencing of L1CAM did not alter primary tumour growth, but increased overall survival of mice. In fact, L1CAM knock down attenuated the formation of liver metastasis more efficiently in the spontaneous (Fig. 2f, ~90 %) than in the experimental metastasis assay (Fig. 3c, ~60 %), which points towards an important role of tumour cell-derived L1CAM for the dissemination of tumour cells from the primary tumour.

Quantitative cell-fate analyses have demonstrated that the early steps in the haematogenous metastatic cascade, including dissemination, are highly efficient. In contrast, at the secondary site only a minority of cancer cells is able to re-initiate proliferation to form micrometastases, and to subsequently grow into macroscopic metastases, making the overall metastatic process inefficient [44, 45]. Whether a tumour cell will grow in a target organ of metastasis is largely dependent on the molecular compatibility of the tumour cell (the seed) with the environment in the specific organ (the soil) in terms of growth factors, specific cell surface receptors or cell adhesion molecules [2]. We found that L1CAM expression was important for tumour cell outgrowth in the target organ of metastasis, which indicates that L1CAM facilitates adaptation of tumour cells to foreign tissues. Since L1CAM is known to prevent apoptosis of tumour cells [46, 47], L1CAM might promote metastasis formation by tipping the proliferation/apoptosis balance to favour metastatic growth. Clinical findings indicate that L1CAM plays an important role during liver metastasis, as in the clinic up to 100 % of melanoma and pancreatic carcinoma liver metastases display high L1CAM levels [28, 48]. Consistently, we here demonstrate that L1CAM is a decisive factor not only for liver metastasis formation, but also for lung metastasis. These observations indicate that the pro-metastatic effect of L1CAM and the underlying mechanisms are not restricted to one specific target organ of metastasis.

Beyond re-initiation of proliferation, tumour cell migration and invasion are prerequisites for efficient metastasis [49, 50] and are strongly dependent on proteolytic activity of matrix-degrading enzymes [3, 9–11, 51]. In fact, elevated L1CAM expression has been located at the invasive front of the tumour tissue in colon, ovarian, and pancreatic carcinoma [34, 52–54], suggesting that L1CAM contributes to the invasive phenotype of these cancers. In line with these findings, we demonstrate that

Fig. 6 L1CAM positively regulates the metastatic potential of ovarian carcinoma cells. SKOV3ip-*lacZ* cells were transduced with retroviruses containing a shRNA sequence directed against human L1CAM (shL1-2) or with a non-targeting shRNA sequence (shscr, scrambled shRNA). **a** TaqMan® analysis revealed significantly reduced L1CAM expression in SKOV3ip-*lacZ* cells. Mean expression of L1CAM mRNA ± SEM (*columns* ± *bars*) in SKOV3ip-*lacZ* cells. L1CAM mRNA expression levels were normalised to 18S rRNA levels and the mean of the reference group (*shscr*) was set as 100 % ($n = 3$ each; shL1-2 vs. shscr: $***p \leq 0.001$, as determined by unpaired *t* test). **b** Western blot analysis revealed that L1CAM protein levels were significantly reduced in SKOV3ip-*lacZ* cells. **c** Flow cytometric analysis revealed that L1CAM expression was significantly reduced in SKOV3ip-*lacZ* cells. **d** Mean number of migrated cells per image section ± SEM (*columns* ± *bars*) for the different SKOV3ip-*lacZ* cells as analysed by Transwell migration assay. Cells were either incubated with 20 μM gelatinase inhibitor SB-3CT or DMSO as a control. The mean of the reference group (*shscr*, *DMSO*) was set as 100 % ($n = 6$ each; all group comparison: $***p \leq 0.001$, as determined by One Way ANOVA; single group comparison: shscr, SB-3CT vs. shscr, DMSO: $***p < 0.001$; shL1-2, DMSO vs. shscr, DMSO: $***p < 0.001$; shL1-2, SB-3CT vs. shscr, DMSO: $***p < 0.001$; shL1-2, SB-3CT vs. shL1-2, DMSO: $**p = 0.002$, as determined by One Way ANOVA and subsequent post hoc comparison by Holm–Sidak method). **e** Mean number of invaded cells per image section ± SEM (*columns* ± *bars*) for the different SKOV3ip-*lacZ* cells as determined by Matrigel Transwell invasion assay. Cells were either incubated with 20 μM gelatinase inhibitor SB-3CT or DMSO as a control. The mean of the reference group (*shscr*, *DMSO*) was set as 100 % ($n = 6$ each; all group comparison: $***p \leq 0.001$, as determined by One Way ANOVA; single group comparison: shscr, SB-3CT vs. shscr, DMSO: $***p < 0.001$; shL1-2, DMSO vs. shscr, DMSO: $***p < 0.001$; shL1-2, SB-3CT vs. shscr, DMSO: $***p < 0.001$; shL1-2, SB-3CT vs. shL1-2, DMSO: $p = 0.242$, as determined by One Way ANOVA and subsequent post hoc comparison by Holm–Sidak method). **f** For analysis of cell viability/proliferation, 2×10^3 cells/well were seeded in 96 well plates, and the number of living cells was quantified 0, 24, 48, 72 and 96 h after seeding using the AlamarBlue® proliferation assay ($n = 6$). **g** Mean expression of MMP-2 mRNA ± SEM (*columns* ± *bars*) in SKOV3ip-*lacZ* cells. MMP-2 mRNA expression levels were normalised to 18S rRNA levels and the mean of the reference group (*shscr*) was set as 100 % ($n = 3$ each; shL1-2 vs. shscr: $***p \leq 0.001$, as determined by unpaired *t*-test). **h** Mean expression of MMP-9 mRNA ± SEM (*columns* ± *bars*) in SKOV3ip-*lacZ* cells. MMP-9 mRNA expression levels were normalised to 18S rRNA levels and the mean of the reference group (*shscr*) was set as 100 % ($n = 3$ each; shL1-2 vs. shscr: $**p = 0.003$, as determined by unpaired *t*-test). **i**, **j** 26 days after inoculation of 1.0×10^5 of the different SKOV3ip-*lacZ* cells, $CD1^{nu/nu}$ mice were sacrificed and their lungs were removed. **i** X-Gal staining (*indigoblue foci*) of removed lungs. Representative surface images are presented (*bars:* 2 mm (macroscopic), 0.2 mm (close-up). **j** Mean number of macrometastases in lungs ± SEM (*columns* ± *bars*). The mean of the reference group (*shscr*) was set as 100 % (shscr: $n = 6$ mice; shL1-2: $n = 10$ mice; shL1-2 vs. shscr: $*p = 0.034$, as determined by Mann–Whitney Rank Sum test)

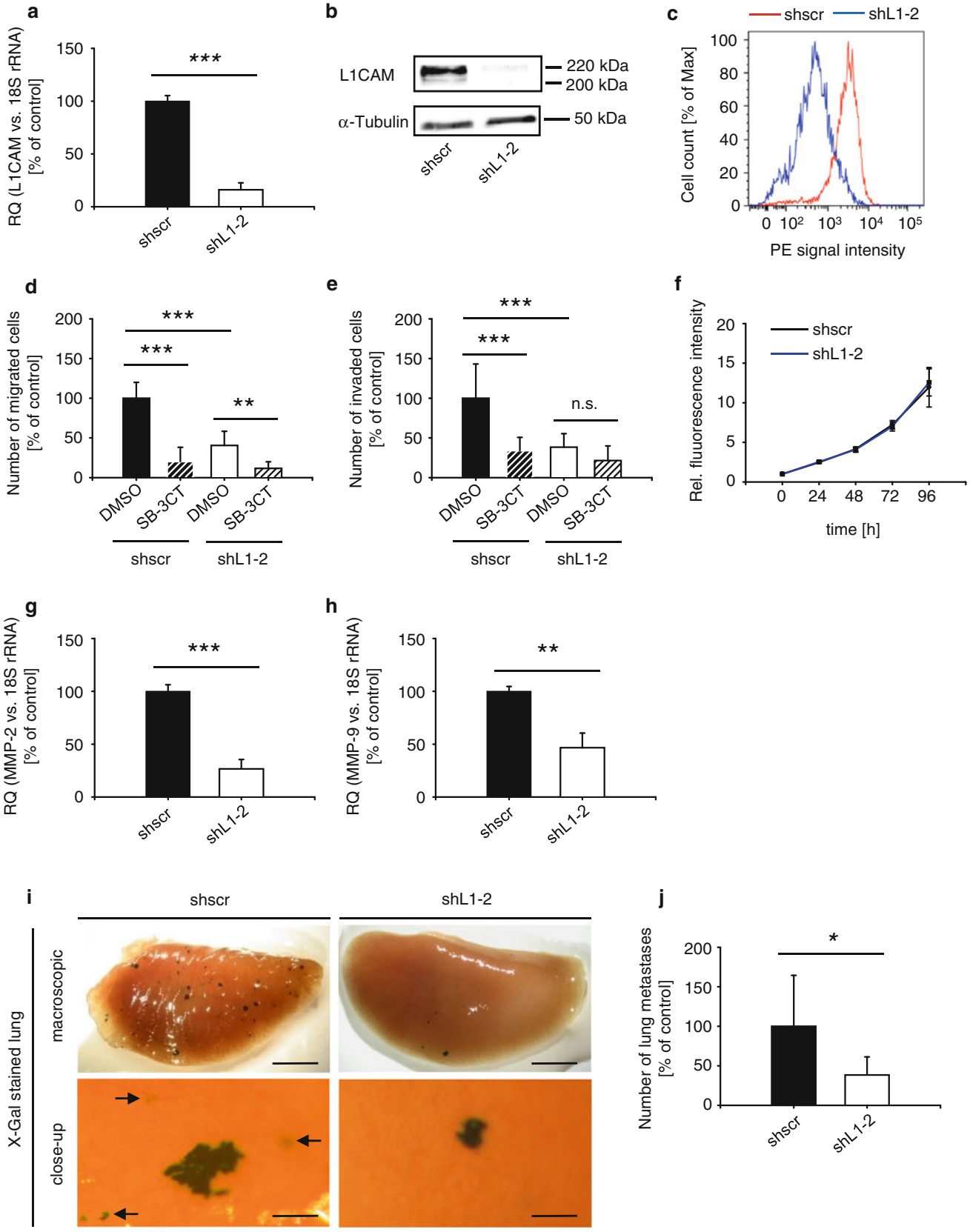
a
RQ (L1CAM vs. 18S rRNA) [% of control]
150
100
50
0
***
shscr
shL1-2
b
L1CAM
220 kDa
200 kDa
α-Tubulin
50 kDa
shscr
shL1-2
c
shscr
shL1-2
Cell count [% of Max]
100
80
60
40
20
0
0 10² 10³ 10⁴ 10⁵
PE signal intensity
d
Number of migrated cells [% of control]
200
150
100
50
0
***
***
**
DMSO
SB-3CT
DMSO
SB-3CT
shscr
shL1-2
e
Number of invaded cells [% of control]
200
150
100
50
0
***
***
n.s.
DMSO
SB-3CT
DMSO
SB-3CT
shscr
shL1-2
f
Rel. fluorescence intensity
20
15
10
5
0
shscr
shL1-2
0 24 48 72 96
time [h]
g
RQ (MMP-2 vs. 18S rRNA) [% of control]
150
100
50
0
***
shscr
shL1-2
h
RQ (MMP-9 vs. 18S rRNA) [% of control]
150
100
50
0
**
shscr
shL1-2
i
shscr
shL1-2
X-Gal stained lung
macroscopic
close-up
j
Number of lung metastases [% of control]
200
150
100
50
0
*
shscr
shL1-2

L1CAM positively regulates mRNA expression of pro-metastatic MMP-2 and MMP-9 in vitro as well as gelatinolytic activity in vivo. Recently, we could show that specific inhibition of MMP-2 and MMP-9 is efficient in blocking liver metastasis [12, 14]. In the present study, we could mimick the effects of L1CAM knock down on metastatic potential of tumour cells by employing the synthetic MMP-2 and MMP-9 inhibitor SB-3CT. Taken together, these findings indicate an interconnection between L1CAM and MMP expression and suggest that these factors cooperate in the promotion of the invasive phenotype. Still, the underlying signalling mechanism requires further investigations in future studies.

In conclusion, our findings that L1CAM promotes tumour cell dissemination, colonization, and outgrowth in the target organ of metastasis via up-regulation of gelatinase expression and via induction of tumour cell proliferation at the site of metastasis, highlight L1CAM as a promising therapy target in the inhibition of metastatic spread of highly aggressive non-solid as well as solid tumours.

Acknowledgments The authors thank Stephanie Hauser, Laura Bickel and Mareike Lehnhoff (all three from Institute for Experimental Oncology and Therapy Research, Klinikum rechts der Isar, Technische Universität München, Germany) for their expert technical support. This work was supported by the Deutsche Forschungsgemeinschaft (Grants KR2047/1-1 and 1-2) to Achim Krüger.

References

1. Sporn MB (1996) The war on cancer. Lancet 347:1377–1381
2. Fidler IJ (2003) The pathogenesis of cancer metastasis: the "seed and soil" hypothesis revisited. Nat Rev Cancer 3:453–458
3. Valastyan S, Weinberg RA (2011) Tumor metastasis: molecular insights and evolving paradigms. Cell 147:275–292
4. Pals ST, de Gorter DJJ, Spaargaren M (2007) Lymphoma dissemination: the other face of lymphocyte homing. Blood 110:3102–3111
5. Noël A, Gutiérrez-Fernández A, Sounni NE et al (2012) New and paradoxical roles of matrix metalloproteinases in the tumor microenvironment. Front Pharmacol 3:140
6. Deryugina EI, Quigley JP (2006) Matrix metalloproteinases and tumor metastasis. Cancer Metastasis Rev 25:9–34
7. Mook ORF, Frederiks WM, Van Noorden CJF (2004) The role of gelatinases in colorectal cancer progression and metastasis. Biochim Biophys Acta 1705:69–89
8. Zeng ZS, Cohen AM, Guillem JG (1999) Loss of basement membrane type IV collagen is associated with increased expression of metalloproteinases 2 and 9 (MMP-2 and MMP-9) during human colorectal tumorigenesis. Carcinogenesis 20: 749–755
9. Dufour A, Zucker S, Sampson NS et al (2010) Role of matrix metalloproteinase-9 dimers in cell migration: design of inhibitory peptides. J Biol Chem 285:35944–35956
10. Dufour A, Sampson NS, Zucker S, Cao J (2008) Role of the hemopexin domain of matrix metalloproteinases in cell migration. J Cell Physiol 217:643–651
11. Chetty C, Vanamala SK, Gondi CS et al (2012) MMP-9 induces CD44 cleavage and CD44 mediated cell migration in glioblastoma xenograft cells. Cell Signal 24:549–559
12. Gerg M, Kopitz C, Schaten S et al (2008) Distinct functionality of tumor cell-derived gelatinases during formation of liver metastases. Mol Cancer Res 6:341–351
13. Brown S, Bernardo M, Li Z-H (2000) Potent and selective mechanism-based inhibition of gelatinases. J Am Chem Soc 122:6799–6800
14. Krüger A, Arlt MJE, Gerg M et al (2005) Antimetastatic activity of a novel mechanism-based gelatinase inhibitor. Cancer Res 65:3523–3526
15. Westermarck J, Kähäri VM (1999) Regulation of matrix metalloproteinase expression in tumor invasion. Faseb J 13: 781–792
16. Munshi HG, Stack MS (2006) Reciprocal interactions between adhesion receptor signaling and MMP regulation. Cancer Metastasis Rev 25:45–56
17. Denzel S, Mack B, Eggert C et al (2012) MMP7 is a target of the tumour-associated antigen EpCAM. Int J Exp Pathol 93:341–353
18. Cavallaro U, Christofori G (2004) Cell adhesion and signalling by cadherins and Ig-CAMs in cancer. Nat Rev Cancer 4:118–132
19. Kiefel H, Bondong S, Hazin J et al (2012) L1CAM: a major driver for tumor cell invasion and motility. Cell Adh Migr 6:374–384
20. Wai Wong C, Dye DE, Coombe DR (2012) The role of immunoglobulin superfamily cell adhesion molecules in cancer metastasis. Int J Cell Biol 2012:340296
21. Gavert N, Ben-Shmuel A, Raveh S, Ben-Ze'ev A (2008) L1-CAM in cancerous tissues. Expert Opin Biol Ther 8:1749–1757
22. Raveh S, Gavert N, Ben-Ze'ev A (2009) L1 cell adhesion molecule (L1CAM) in invasive tumors. Cancer Lett 282:137–145
23. Fogel M, Gutwein P, Mechtersheimer S et al (2003) L1 expression as a predictor of progression and survival in patients with uterine and ovarian carcinomas. Lancet 362:869–875
24. Schäfer H, Geismann C, Heneweer C et al (2012) Myofibroblast-induced tumorigenicity of pancreatic ductal epithelial cells is L1CAM dependent. Carcinogenesis 33:84–93
25. Gavert N, Sheffer M, Raveh S et al (2007) Expression of L1-CAM and ADAM10 in human colon cancer cells induces metastasis. Cancer Res 67:7703–7712
26. Gavert N, Ben-Shmuel A, Lemmon V et al (2010) Nuclear factor-kappaB signaling and ezrin are essential for L1-mediated metastasis of colon cancer cells. J Cell Sci 123:2135–2143
27. Gavert N, Vivanti A, Hazin J et al (2011) L1-mediated colon cancer cell metastasis does not require changes in EMT and cancer stem cell markers. Mol Cancer Res 9:14–24
28. Thies A, Schachner M, Moll I et al (2002) Overexpression of the cell adhesion molecule L1 is associated with metastasis in cutaneous malignant melanoma. Eur J Cancer 38:1708–1716
29. Arlt MJE, Novak-Hofer I, Gast D et al (2006) Efficient inhibition of intra-peritoneal tumor growth and dissemination of human ovarian carcinoma cells in nude mice by anti-L1-cell adhesion molecule monoclonal antibody treatment. Cancer Res 66: 936–943
30. Fischer E, Grünberg J, Cohrs S et al (2012) L1-CAM-targeted antibody therapy and (177)Lu-radioimmunotherapy of disseminated ovarian cancer. Int J Cancer 130:2715–2721
31. Knogler K, Grünberg J, Zimmermann K et al (2007) Copper-67 radioimmunotherapy and growth inhibition by anti-L1-cell adhesion molecule monoclonal antibodies in a therapy model of ovarian cancer metastasis. Clin Cancer Res 13:603–611
32. Hai J, Zhu C-Q, Bandarchi B et al (2012) L1 cell adhesion molecule promotes tumorigenicity and metastatic potential in non-small cell lung cancer. Clin Cancer Res 18:1914–1924

33. Hung S-C, Wu I-H, Hsue S-S et al (2010) Targeting l1 cell adhesion molecule using lentivirus-mediated short hairpin RNA interference reverses aggressiveness of oral squamous cell carcinoma. Mol Pharm 7:2312–2323
34. Krüger A, Schirrmacher V, von Hoegen P (1994) Scattered micrometastases visualized at the single-cell level: detection and re-isolation of lacZ-labeled metastasized lymphoma cells. Int J Cancer 58:275–284
35. Soneoka Y, Cannon PM, Ramsdale EE et al (1995) A transient three-plasmid expression system for the production of high titer retroviral vectors. Nucleic Acids Res 23:628–633
36. Yee JK, Miyanohara A, LaPorte P et al (1994) A general method for the generation of high-titer, pantropic retroviral vectors: highly efficient infection of primary hepatocytes. Proc Natl Acad Sci USA 91:9564–9568
37. Kopitz C, Anton M, Gansbacher B, Krüger A (2005) Reduction of experimental human fibrosarcoma lung metastasis in mice by adenovirus-mediated cystatin C overexpression in the host. Cancer Res 65:8608–8612
38. Krüger A, Umansky V, Rocha M et al (1994) Pattern and load of spontaneous liver metastasis dependent on host immune status studied with a lacZ transduced lymphoma. Blood 84:3166–3174
39. Arlt M, Kopitz C, Pennington C et al (2002) Increase in gelatinase-specificity of matrix metalloproteinase inhibitors correlates with antimetastatic efficacy in a T-cell lymphoma model. Cancer Res 62:5543–5550
40. Wolterink S, Moldenhauer G, Fogel M et al (2010) Therapeutic antibodies to human L1CAM: functional characterization and application in a mouse model for ovarian carcinoma. Cancer Res 70:2504–2515
41. Gast D, Riedle S, Riedle S et al (2005) L1 augments cell migration and tumor growth but not beta3 integrin expression in ovarian carcinomas. Int J Cancer 115:658–665
42. Gast D, Riedle S, Issa Y et al (2008) The cytoplasmic part of L1-CAM controls growth and gene expression in human tumors that is reversed by therapeutic antibodies. Oncogene 27:1281–1289
43. Zhang H, Wong CCL, Wei H et al (2012) HIF-1-dependent expression of angiopoietin-like 4 and L1CAM mediates vascular metastasis of hypoxic breast cancer cells to the lungs. Oncogene 31:1757–1770
44. Chambers AF, Groom AC, MacDonald IC (2002) Dissemination and growth of cancer cells in metastatic sites. Nat Rev Cancer 2:563–572
45. Luzzi KJ, MacDonald IC, Schmidt EE et al (1998) Multistep nature of metastatic inefficiency: dormancy of solitary cells after successful extravasation and limited survival of early micrometastases. Am J Pathol 153:865–873
46. Sebens Müerköster S, Werbing V, Sipos B et al (2007) Drug-induced expression of the cellular adhesion molecule L1CAM confers anti-apoptotic protection and chemoresistance in pancreatic ductal adenocarcinoma cells. Oncogene 26:2759–2768
47. Stoeck A, Gast D, Sanderson MP et al (2007) L1-CAM in a membrane-bound or soluble form augments protection from apoptosis in ovarian carcinoma cells. Gynecol Oncol 104: 461–469
48. Bergmann F, Wandschneider F, Sipos B et al (2010) Elevated L1CAM expression in precursor lesions and primary and metastastic tissues of pancreatic ductal adenocarcinoma. Oncol Rep 24:909–915
49. Friedl P, Alexander S (2011) Cancer invasion and the microenvironment: plasticity and reciprocity. Cell 147:992–1009
50. Yilmaz M, Christofori G (2010) Mechanisms of motility in metastasizing cells. Mol Cancer Res 8:629–642
51. Björklund M, Koivunen E (2005) Gelatinase-mediated migration and invasion of cancer cells. Biochim Biophys Acta 1755:37–69
52. Gavert N, Conacci-Sorrell M, Gast D et al (2005) L1, a novel target of beta-catenin signaling, transforms cells and is expressed at the invasive front of colon cancers. J Cell Biol 168:633–642
53. Tsutsumi S, Morohashi S, Kudo Y et al (2011) L1 Cell adhesion molecule (L1CAM) expression at the cancer invasive front is a novel prognostic marker of pancreatic ductal adenocarcinoma. J Surg Oncol 103:669–673
54. Zecchini S, Bianchi M, Colombo N et al (2008) The differential role of L1 in ovarian carcinoma and normal ovarian surface epithelium. Cancer Res 68:1110–1118